Heliyon 10 (2024) e26836

Contents lists available at ScienceDirect

Heliyon

journal homepage: www.cell.com/heliyon

Research article

Assessment of sepsis-associated encephalopathy by quantitative magnetic resonance spectroscopy in a rat model of cecal ligation and puncture☆

Siqi Liu [a,1], Zhifeng Liu [b,1], Gongfa Wu [b,1], Haoyi Ye [b], Zhihua Wu [b], Zhengfei Yang [a,*], Shanping Jiang [a,**]

[a] Sun Yat-sen Memorial Hospital, Sun Yat-sen University, Guangzhou, 510120, China
[b] The Fourth Affiliated Hospital of Guangzhou Medical University, Guangzhou, 511300, China

ARTICLE INFO

Keywords:
Sepsis
Cecal ligation and puncture
Brain injury
1H-MRS
Neurological deficit

ABSTRACT

Proton magnetic resonance spectroscopy (1H-MRS) is the only non-invasive technique to quantify neurometabolic compounds in the living brain. We used 1H-MRS to evaluate the brain metabolites in a rat model of Sepsis-associated encephalopathy (SAE) established by cecal ligation and puncture (CLP). 36 male Sprague-Dawley rats were randomly divided into sham and CLP groups. Each group was further divided into three subgroups: subgroup O, subgroup M, and subgroup N. Neurological function assessments were performed on the animals in the subgroup O and subgroup N at 24 h, 48 h, and 72 h. The animals in the subgroup M were examined by magnetic resonance imaging (MRI) at 12 h after CLP. Compared with the sham group, the ratio of N-acetylaspartate (NAA) to creatine (Cr) in the hippocampus was significantly lower in the CLP group. The respective ratios of lactate (Lac), myo-inositol (mIns), glutamate and glutamine (Glx), lipid (Lip), and choline (Cho) to Cr in the CLP group were clearly higher than those in the sham group. Cytochrome *c*, intimately related to oxidative stress, was elevated in the CLP group. Neurofilament light (NfL) chain and glial fibrillary acidic protein (GFAP) scores in the CLP group were significantly higher than those in the sham group, while zonula occludens-1 (ZO-1) was downregulated. Compared with the sham group, the CLP group displayed higher values of oxygen extraction fraction (OEF), central venous–arterial partial pressure of carbon dioxide (P (cv-a) CO2), and central venous lactate (VLac). In contrast, jugular venous oxygen saturation (SjvO2) declined. In the present study, 1H-MRS could be used to quantitatively assess brain injury in terms of microcirculation disorder, oxidative stress, blood–brain barrier disruption, and glial cell activation through changes in metabolites within brain tissue.

1. Introduction

Sepsis, a dysregulated host response to infection, is a form of life-threatening organ dysfunction [1]. The central nervous system is

☆ The experiments were performed in Sun Yat-sen Memorial Hospital.

* Corresponding author. Sun Yat-sen Memorial Hospital of Sun Yat-sen University, 107 Yan Jiang Xi Road, Guangzhou, 510120, China.
** Corresponding author. Sun Yat-sen Memorial Hospital of Sun Yat-sen University, 107 Yan Jiang Xi Road, Guangzhou, 510120, China.
E-mail addresses: yangzhengfei@vip163.com (Z. Yang), jiangshp@mail.sysu.edu.cn (S. Jiang).

[1] These authors contributed equally to this work.

https://doi.org/10.1016/j.heliyon.2024.e26836
Received 23 July 2023; Received in revised form 6 February 2024; Accepted 20 February 2024
Available online 22 February 2024

one of the most vulnerable organ systems in a particular type of sepsis known as sepsis-associated encephalopathy (SAE) [2,3]. The prevalence of SAE ranges from 30% to 70%, with increased mortality and risk of long-term cognitive impairment, mainly due to neuroinflammation, oxidative stress, alterations in cerebral perfusion and metabolism, and blood–brain barrier disruption [2,4].

Unfortunately, with its insidious early symptoms, SAE is difficult to recognize because of the non-specific clinical manifestations and the application of sedation [5]. Various approaches can be used to assess SAE, such as clinical feature scoring, electroencephalogram (EEG) analysis, and somatosensory evoked potential (SSEP) measurement [6]. Yet those methods are highly subjective and of low specificity, which limit their broader utility in the clinic [2,7].

Accumulating evidence has suggested that magnetic resonance imaging (MRI) can accurately detect SAE at an early stage [2]. Magnetic resonance spectroscopy (MRS) is a quantitative, non-invasive MR technique that measures brain metabolites in vivo [8]. The altered metabolism of the brain may be the critical trigger of SAE [3]. Based on the work of Bozza and colleagues, proton (1H) MRS has focused on the absolute concentrations of metabolites such as N-acetylaspartate (NAA), creatine (Cr), and choline (Cho) in a rat model of sepsis induced by cecal ligation and puncture (CLP), as well as the ratios of those concentrations. They found neuronal injury accompanied by decreased NAA levels in SAE [9]. NAA is a marker of neuronal mitochondrial function, the level of which is reduced in ischemic stroke, brain injury, and SAE [9–11]. Cho is regarded as a marker of inflammation and gliosis [12]. Cr is related to cerebral energy metabolism [13]. In addition, MRS studies on traumatic brain injury and hypoxic ischemic encephalopathy have shown that other metabolites are also detectable, such as lactate (Lac), myo-inositol (mIns), glutamate and glutamine (Glx), lipid (Lip) and citrate (Ci) [11]. According to Li et al. [14]. cognitive deficits were positively associated with high values for the amplitudes of low-frequency fluctuations (ALFF), the Glx/Cr ratio, and the mIns/Cr ratio in the hippocampus of brains subject to SAE. It has been proven that microcirculatory dysfunction is implicated in the pathogenesis of SAE [15]. Lac and Ci, important intermediate products of energy metabolism, are abnormally elevated during microcirculatory disorder [16,17]. The metabolite mIns is found mainly in astrocytes and microglial cells, which maintain osmotic pressure. Glx denotes glutamate and glutamine and is associated with poor long-term prognosis in traumatic brain injury [18]. Higher levels of mIns and Lip have been correlated with an elevated concentration of macrophages, and glutamate excitotoxicity has been associated with many acute and chronic neurological disorders [18–20]. Significant differences in the above indicators might therefore be detected by MRS in the early stages of SAE.

In the present study we aimed to investigate whether MRS could provide early detection of the accumulation of multiple metabolites in a rat model of CLP-induced SAE. We also sought to find some additional evidence to elucidate the underlying mechanisms of alterations in brain metabolites through modifications in observations from blood gas analysis, markers of neurological damage in the brain, and plasma cytokine. This study provided an experimental basis to use MRS as a promising tool for predicting and assessing cerebral dysfunction in sepsis patients.

2. Materials and methods

2.1. Ethics statement

This experimental protocol-including use of induced anesthesia, anesthesia method, surgical procedures and experimental procedures — was approved by the Institutional Animal Care and Use Committee of Sun Yat-sen Memorial Hospital *(SYSU-IACUC-2023-B0014)*. All animals were cared for humanely and handled in compliance with the Guide for the Care and Use of Laboratory Animals published by the US National Institutes of Health and the "Principles of Laboratory Animal Care" [21,22]. All efforts aimed to minimize suffering.

2.2. Animal preparation

A total of 36 healthy male Sprague-Dawley rats, with masses between 200 g and 250 g, were obtained from the Laboratory Animal Center of Sun Yat-sen University. They were acclimatized and fed for seven days before the surgery and fasted overnight. All rats first underwent inhalation anesthesia with carbon dioxide for 10 s, followed by intraperitoneal anesthesia with 45 mg/kg of 3% sodium pentobarbital.

2.3. Experimental procedures

The rats were randomly divided into the sham group and the CLP group. Each group was further divided into three subgroups ($n = 6$ per subgroup): subgroup O (underwent the open-field test at 24 h, 48 h, and 72 h), subgroup N (the neurological deficit score (NDS) were performed at 24 h, 48 h, and 72 h), and subgroup M (examined by MRI at 12 h after CLP). The abdominal surgical area of all rats was then shaved and disinfected. A longitudinal incision (2 cm) was made along the midline to open the abdomen. Rats in the sham group only underwent laparotomy, and the belly was sutured layer by layer. The CLP group underwent cecal ligation and puncture. In particular, we separated the distal cecum and tightly ligated approximately one third of the cecum with a 3-0 silk suture. We then punctured the ligated end of the cecum with an 18-gauge needle, and a small number of feces were squeezed and smeared through the puncture hole into the peritoneal cavity. Finally, the abdomen was closed by suturing the muscle and skin [23].

The animals in the subgroups O underwent the open-field test at 24 h, 48 h, and 72 h. The animals in the subgroup N underwent the neurological deficit score (NDS) assessments at 24 h, 48 h and 72 h. The animals in the subgroups M underwent an MRI examination at 12 h after CLP. A PE-50 catheter was inserted into the right internal jugular vein and left femoral artery to draw blood samples. After undergoing an MRI scan and blood sampling from the right internal jugular vein and left femoral artery, the rats in the two subgroup M

were sacrificed, and their brains were harvested for histological examination.

2.4. Functional neurological examination

2.4.1. The neurological deficit score (NDS)

The severity of the neurological deficit was evaluated at 24, 48 and 72 h post-operation according to the neurological deficit score (NDS). The neurological deficit score consists of seven items and a total score from 0 (normal function) to 500 (maximal deficit). The neurological deficit score consists of seven items: level of consciousness, respiration, cornea reflex, cranial reflex or gag reflex, auditory reflex, motor sensory function, and behavior, respectively [24].

2.4.2. The open-field test

As previously described, the open field test evaluated the motor function and exploratory locomotion [25]. Individual rats were placed in a plastic chamber (100 × 100 × 100 cm, item # 63007, RWD, Life Science Co., Ltd, Shenzhen, China) designed with computer-controlled photocells. Each rat was positioned at a consistent starting point and allowed to explore the apparatus for 5 min. The open field arena was sanitized with 70% ethanol following each test. The movements of the animals were captured by a video camera (64088, RWD, Life Science Co., Ltd, Shenzhen, China) positioned above the apparatus and subsequently analyzed using SMART 3.0 software (RWD, Life Science Co., Ltd, Shenzhen, China). The software analyzed the total distance traveled, track maps, and the number of zone transition by the animal during the 5-min recording time.

2.5. MRI scan protocol and in vivo proton spectroscopy

Rats were scanned by 3.0 T superconducting MRI (Prisma, Siemens), using an 80 mT/s gradient magnetic field with a maximum gradient slew rate of 200 T/m/s and an 8-channel rodent-specific coil (Mouse Coil-M, CL33000001). MRS was performed using Siemens chemical-shift imaging with the following settings: echo time (TE) = 35 ms; acquisition = 4 times; bandwidth = 1200 Hz/px; average = 80; and MRS single voxel acquisition size = 4 × 5 × 5 $mm.^3$ The volume of interest (VOI) was placed in the unilateral hippocampus. We placed the spectroscopy VOI in the same position for each session based on the type of lesion and the anatomical landmarks [10].

The acquired MRS image data were processed on a Siemens post-processing workstation. MRS measured the relative quantitative values of metabolites within VOI: N-acetylaspartate (NAA peak, 2.02 ppm), creatine (Cr peak, 3.05 ppm), choline (Cho peak, 3.20 ppm), lactate (Lactate peak, 1.31 ppm), glutamate and glutamine (Glx peak, 3.76 ppm), myo-inositol (mIns peak, 3.52 ppm), and citrate (Ci peak, 2.60 ppm). Normalized values were calculated to eliminate the differences among individuals (NAA/Cr, Cho/Cr, Lac/Cr, Glx/Cr, mIns/Cr, and Ci/Cr).

2.6. Serum biochemical arrays

Blood samples were collected through a PE-50 catheter using an aseptic technique. After centrifugation (3000 *g*, 10 min), serum was separated and stored at −80 °C for further analysis. Serum IL-1β, IL-6, IL-10 and TNF-α assays were conducted using specific enzyme-linked immunoassay kits (all from Abcam Biotechnology, Cambridge, USA) following the manufacturer's protocol.

2.7. Histopathology and immunohistochemistry

Animals were sacrificed after MRI examination, and brain tissue samples were harvested for histological and immunohistochemical analysis. After formalin fixation, fresh harvested brain samples were paraffin-embedded and sectioned before hematoxylin and eosin (H&E) staining. Staining for neurofilament light (NfL) chain, glial fibrillary acidic protein (GFAP), zonula occludens-1 (ZO-1), and cytochrome *c* (Cyt C), was executed using a Max Vision Super HRP IHC Kit (Kit9922), following the manufacturer's recommended protocol. Immunohistochemical image quantitation was conducted in Image-Pro Plus 6.0 software by two pathologists blinded to the rats' group assignment.

2.8. Blood gas analysis

In order to obtain indicators of cerebral microcirculation and systemic microcirculation, at baseline, and 12 h post-CLP, venous blood and arterial blood were withdrawn in 0.2 mL samples. The blood gas indices [pH, partial pressure of oxygen (PaO_2), partial pressure of carbon dioxide ($PaCO_2$), arterial oxygen saturation (SaO_2), jugular venous oxygen saturation ($SjvO_2$) and lactate] were determined by use of an iSTAT blood gas analyzer (Abbott, USA; CG4+ cartridge). The central venous-to-arterial difference in carbon dioxide partial pressure [P (cv-a) CO_2] was calculated as the difference between jugular venous $PaCO_2$ and arterial $PaCO_2$. The oxygen extraction fraction (OEF) was calculated using the equation $OEF = (1 - SjvO_2/SaO_2) \times 100\%$ [26].

2.9. Statistical analysis

The IBM SPSS Statistics version 25.0 software package (IBM, Armonk, USA) was used for the statistical analysis. Continuous variables were expressed as mean ± standard deviation (SD) and analyzed by *t*-test between both groups of independent samples. A

two-tailed $p < 0.05$ was considered statistically significant.

3. Results

3.1. Baseline characteristics of rats

A total of 36 rats were utilized in this study: 18 rats underwent CLP, and 18 rats received a sham operation. There were no statistically significant differences in body mass, baseline hemodynamics, or physiological parameters between the two groups (Table 1). Table 1 illustrates the consistency in the baseline characteristics of the original samples.

3.2. Neurological outcome after CLP

3.2.1. The NDS value

The NDS value for the sham group was 0. For the CLP subgroup N the NDS gradually increased with time after exposure to CLP (Table 2), revealing that sepsis induces cognitive dysfunction and neurological injury in CLP rats.

3.2.2. The open field test

Rats subjected to CLP, the CLP subgroup O, exhibited decreased total distance traveled and the number of zone transition compared to the sham subgroup O rats, suggesting that sepsis induces a decline in exploratory activity and triggers anxious behavior in the rat subjects (Fig. 1A–C).

3.3. Sepsis induces overexpression of inflammatory cytokines

Rats that underwent CLP, the CLP subgroup M, had higher proinflammatory cytokines (IL-1β, IL-6, TNF-α) and anti-inflammatory IL-10 than the sham subgroup M rats (Fig. 2), suggesting that sepsis drives an excessive systemic inflammatory response and immune response.

3.4. 1H-MRS-based metabolite profile

Absolute concentrations of metabolites in the unilateral hippocampus of rats were quantified by 1H MRS (Fig. 3A and B). Cr did not differ between the two groups (Fig. 3C). Compared to the sham subgroup M, the NAA/Cr ratio in the CLP-induced sepsis subgroup M decreased to a statistically significant extent (Fig. 3D), suggesting possible structural and functional dysfunction of hippocampal neurons. Several relative metabolite concentrations — Lac/Cr, Cho/Cr, mIns/Cr, Lip/Cr, and Glx/Cr — were elevated to varying degrees (Fig. 3E–I). The results suggested that sepsis leads to impaired cerebral microcirculation, neuroinflammation, glial cell proliferation, and reduced blood-brain barrier integrity. There were no between-group differences for Ci/Cr (Fig. 3J).

3.5. Histopathological analysis and immunohistochemical score

Histopathological evaluation revealed no signs of brain tissue disorders, inflammatory cell infiltration, edema, or neuronal degeneration in the two groups. Cyt C, NfL, GFAP scores were dramatically higher in the CLP subgroup M than in the sham subgroup M, revealing that sepsis drives mitochondrial damage, axonal damage and astrocyte activation in brain tissue, which play an important role in SAE. The ZO-1 expression in the brain tissue of the model group was significantly lower than that of the sham subgroup M (Fig. 4), indicating that sepsis leads to a compromise in the integrity of the blood–brain barrier (BBB).

3.6. Sepsis exacerbates cerebral oxygen metabolism disorder

To explore the effects of sepsis on cerebral oxygen metabolism, internal jugular vein and peripheral arterial blood gas were analyzed. Compared with the sham subgroup M, SjvO2 in the CLP subgroup M was significantly lower ($p < 0.05$, Fig. 5A). However,

Table 1
Baseline physiological parameters of sham group and CLP 12 h group.

Variables	Sham	CLP	*p*
Body weight, g	230 ± 10	222 ± 16	NS
Heart rate, bpm	328 ± 18	334 ± 19	NS
Temperature, °C	37.0 ± 0.3	37.1 ± 0.4	NS
PaO_2	85 ± 9	81 ± 8	NS
Lactate, mmol/L	1.1 ± 0.5	1.2 ± 0.4	NS
pH	7.42 ± 0.08	7.45 ± 0.07	NS

Values are presented as mean ± SD. CLP denotes cecum ligation and puncture. NS denotes no statistical significance. Baseline physiological parameters and blood gas analytical measurements did not show a statistically significant difference between the two groups (all $p > 0.05$).

Table 2
Comparison of neurological deficit scores (NDS) between sham NDS sub group and CLP NDS subgroup.

Time	Sham	CLP	*p*
24 h	0	183 ± 39	<0.01
48 h	0	233 ± 30	<0.01
72 h	0	282 ± 26	<0.01

Values are presented as mean ± SD.

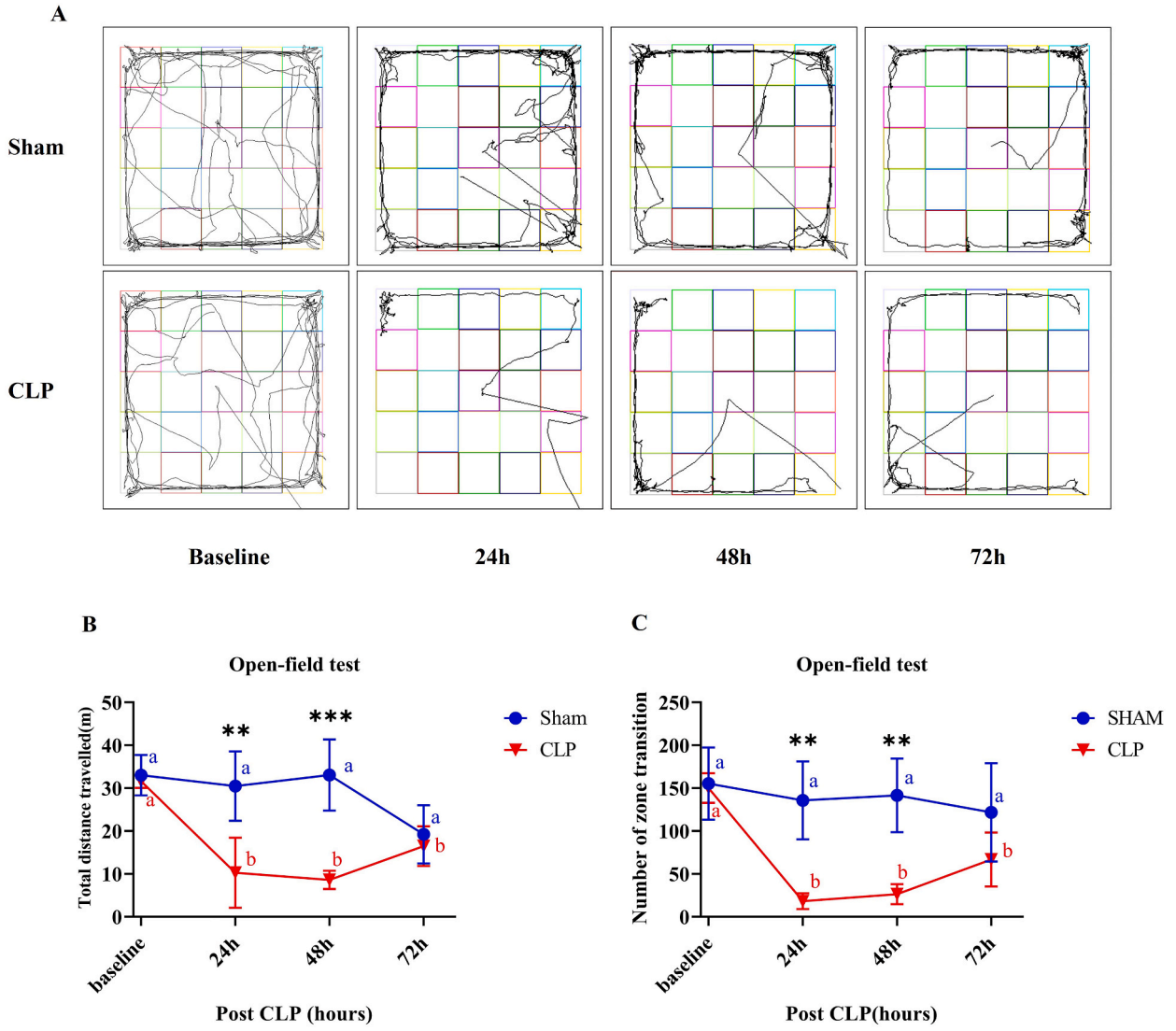

Fig. 1. Open-field test results for the subgroups O of the sham and CLP. **(A)** Representative tracking maps in the open field chamber of the different time-point in the two groups. **(B)** Comparison of the total distance traveled and **(C)** the number of zone transition between the two groups at different time. Note: CLP denotes cecal ligation and puncture. Time-points with different letters differ significantly (ab, $*p < 0.05$). $**p < 0.01$. $***p < 0.001$ compared to the sham group.

the CLP subgroup M displayed high levels of OEF, P (cv-a) CO_2, and VLac 12 h after CLP, compared with the sham subgroup M ($p < 0.05$, Fig. 5B–D), suggesting dysfunction of cerebral microcirculation.

4. Discussion

In this study, we found early changes manifested in MRS in a rat model of CLP-induced SAE. Specifically, hippocampus MRS

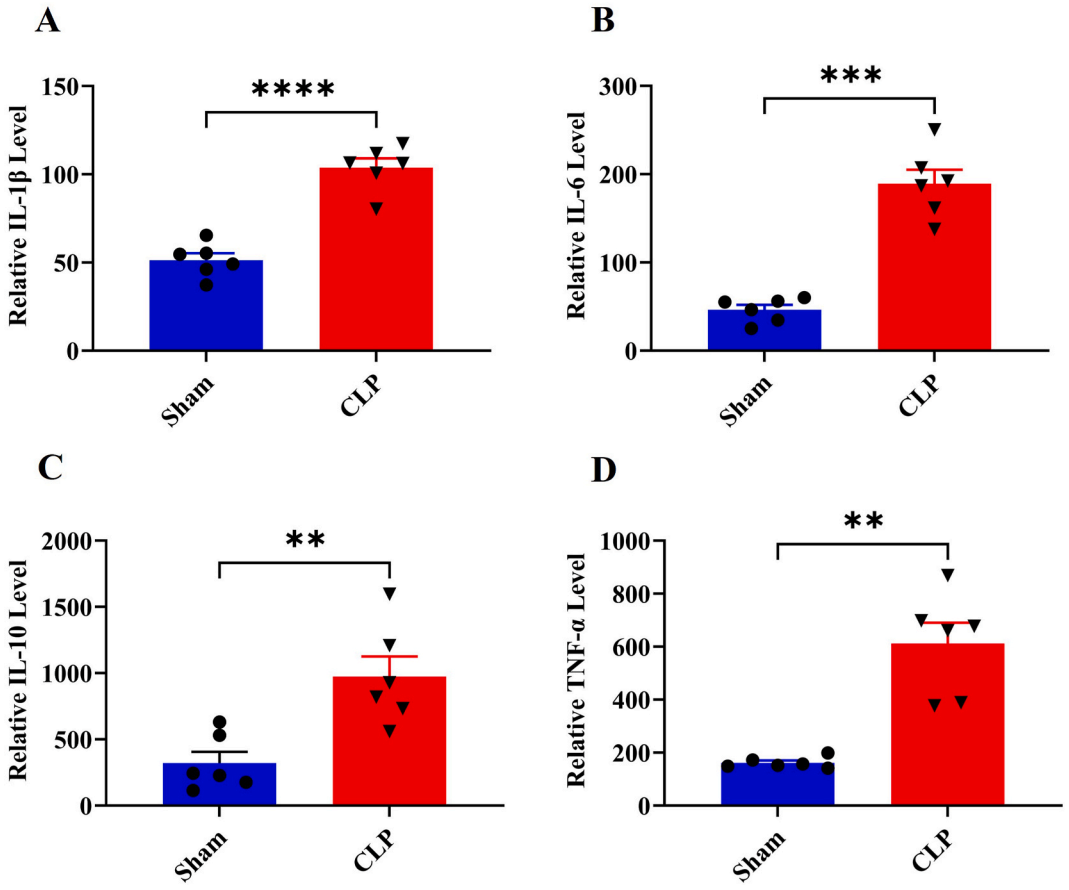

Fig. 2. Changes in inflammatory cytokines in rat plasma, as evident in the relative expression of (A) IL-1β, (B) IL-6, (C) IL-10, and (D) TNF-α. Note: CLP denotes cecal ligation and puncture. *$p < 0.05$. **$p < 0.01$. ***$p < 0.001$. ****$p < 0.0001$.

measurements of neurometabolic alteration, such as NAA/Cr, Lac/Cr, Cho/Cr, Glx/Cr, Lip/Cr, and mIns/Cr, were already apparent as early as 12 h after CLP and preceded the morphological alterations. In view of this, several indicators were measured to validate the corresponding changes in molecular biology and microcirculation, which were consistent with the results of MRS.

The identification of SAE by MRS has been verified in several studies. Previous evidence suggested that the relative concentrations of cerebral Cho, Cr, and NAA measured by MRS had been associated with neurological outcomes [8,9,11,27]. The Cho peak in 1H MRS is also influenced by glycerophosphorylcholine, phosphocholine, and phosphatidylcholine [28]. Because changes in Cho reflect non-homeostatic changes in membrane turnover, as seen in tumors, inflammation, Alzheimer's disease, etc. Free choline levels are elevated when the brain's energy supply is impaired. Free choline concentration correlates best with Cho resonance. Cho peak area is assumed to be a marker of inflammation and gliosis [12]. NAA, regarded as a marker of neuronal mitochondrial function [29], is synthesized from aspartate and acetyl-coenzyme A in neuronal mitochondria and has been found in reduced concentrations in various diseases associated with neuronal damage [30], such as ischemic stroke, brain injury, and brain tumors [10,11,31]. Thus, reduction of NAA can be due to both neuron loss and altered function, associated with poor neurological outcomes [27]. Therefore, it can be inferred that sepsis can lead to neuronal mitochondrial dysfunction in the hippocampus, which affects energy metabolism. The concentration of Cr remains relatively constant across diverse models [32]. Because of this, Cr is used as an internal standard in MRS [32]; however, it may be disturbed by mitochondrial dysfunction in sepsis [16]. In the present study, no differences in Cr were observed between the two groups. Therefore, other metabolites' concentrations were normalized by the Cr level. Statistically significant differences between the two groups could be found in NAA/Cr and Cho/Cr. NAA/Cr was diminished, and Cho/Cr increased, in agreement with previous studies [8,9].

The ratio of myo-inositol (mIns) concentration over creatine concentration showed a unilateral increase in the hippocampus in this study. mIns is an osmolyte found mainly in astrocytes and microglial cells. Previous studies have detected elevated mIns through 1H-MRS in both human and rat models of brain injury, with the primary mechanism being proliferation of reactive astrocytes and microglia [18]. Glial cell activation is a crucial effector of the CNS immune response and indicates the presence of inflammatory signals. Our results support the rapid activation of both microglial cells and astrocytes accompanying the occurrence and progression of SAE [33].

In addition, immunohistochemistry markers, NfL levels, and GFAP expression were significantly higher in the CLP group, which

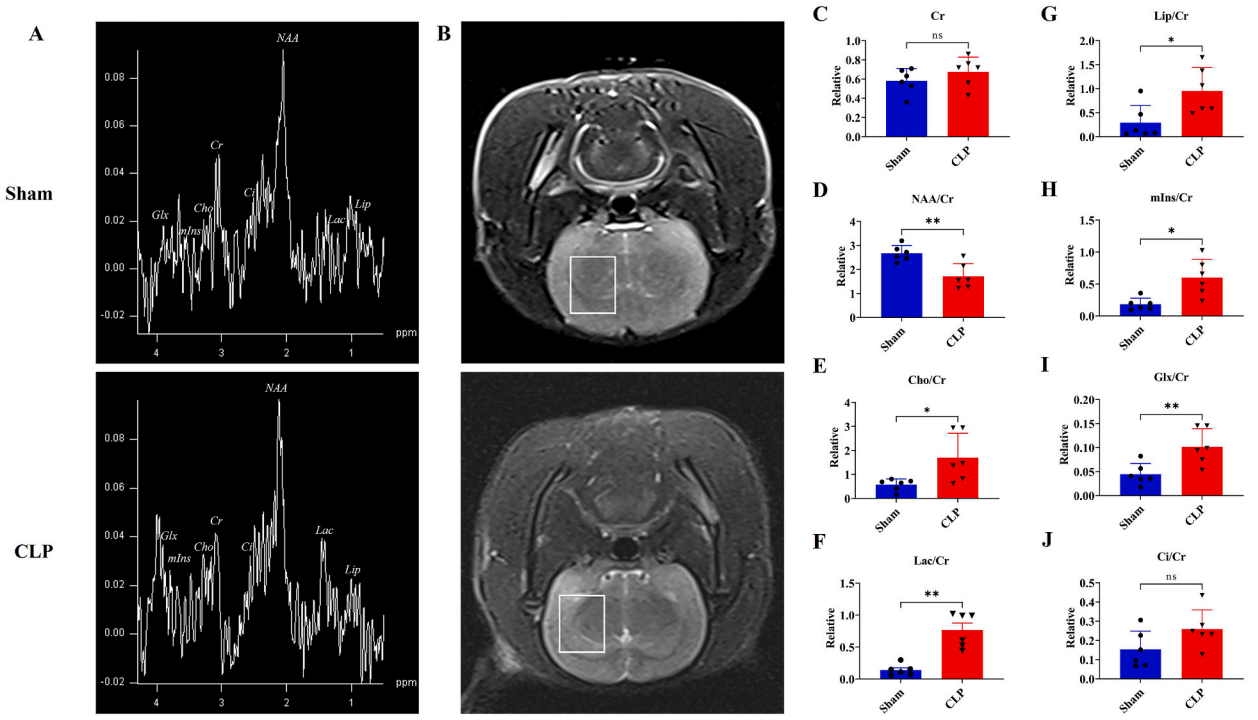

Fig. 3. 1H spectroscopic analysis of brain metabolites and volume of interest (VOI) of the hippocampal region in the subgroups M of the sham and CLP. (A) Representative spectrum of the unilateral hippocampus, with the metabolic peaks identified as NAA, Cr, Cho, Lac, mIns, Glx, Ci and Lip. Quantitative analysis of the absolute and relative concentrations of the different metabolites in the two groups, comprising **(C)**Cr, **(D)** NAA/Cr, **(E)** Cho/Cr, **(F)** Lac/Cr, **(G)** Lip/Cr, **(H)** mIns/Cr, **(I)** Glx/Cr, and **(J)** Ci/Cr. **(B)** Representative VOI of the hippocampal region in the two groups (VOI is indicated by a white box). Note: CLP = cecal ligation and puncture; NAA = N-acetylaspartate; Cr = creatine; Cho = choline, Lac = lactate; mIns = myo-inositol; Glx = glutamate and glutamine; Ci = citrate; and Lip = lipid. *$p < 0.05$. **$p < 0.01$.

validated the results mentioned above. NfL, released into the extracellular space when axons are damaged, is one of the major structural components of the neuronal cytoskeleton [34]. NfL is considered a sensitive biomarker of axonal damage [35]. GFAP, known as an intermediate filament protein, explicitly exists in astrocytes in the brain [36]. Elevated levels of brain and serum GFAP in CNS injuries play a crucial role in astrocyte activation [36]. Previous studies indicated that GFAP expression was significantly increased in sepsis, hemorrhagic stroke, and ischemic stroke [36,37]. Our immunohistochemical results illustrated that sepsis causes damage to CNS neurons, so NfL is released extracellularly with elevated expression. Also, sepsis induces astrocyte proliferation, so GFAP expression was elevated in brain tissue. The above results were consistent with the MRS results. In summary, metabolites measured via MRS showed pathophysiological changes due to SAE.

Microcirculatory disorders are the driver of sepsis and induce excitotoxicity [38,39]. Glutamate is an excitatory central neurotransmitter that is interconverted with glutamine. Glial cells are activated to produce excitotoxicity by increasing glutamate release [18]. The elevated Glx/Cr ratio in the current study confirmed the presence of these alterations in the hippocampus during the early stages of sepsis. During pathophysiological conditions there is a supply–demand imbalance of energy and an impaired ability to mediate phosphorylation, leading to an increase in lactate concentration, which often precedes cellular damage and can be used as an indicator to assess energy failure of the brain [40]. MRS detection of lactate in the CNS facilitated the diagnosis of mitochondrial disease [41]. Upon mitochondrial damage Cyt C is released into the cytoplasm to initiate apoptosis [9], and the tricarboxylic acid cycle is blocked [42]. The Lac peak and the immunohistochemical results of Cyt C were significantly higher in the hippocampal region of rats in the CLP group, which demonstrated that the Lac peak of MRS in CLP-group rats was able to reflect the metabolic changes caused by mitochondrial injury. The Lac peak in MRS and the Cyt C results therefore suggest cerebral microcirculation disorders and mitochondrial damage caused by oxidative stress in the early stage of SAE. In this study, results from arteriovenous blood gas analysis support the occurrence of microcirculatory disturbance in the rat model of CLP. Most of the jugular vein bulb blood is from the intracranial venous systems, so its oxygen saturation and lactate content reveal whole-brain perfusion and cerebral oxygen metabolism [43]. Compared with the sham group, the lactate content of the internal jugular vein bulb, oxygen extraction fraction (OEF), and P (cv-a) CO_2 were markedly elevated in CLP-group rats. Hyperlactatemia together with high P (cv-a) CO_2 or low $SjvO_2$ suggest a worse circulatory dysfunction with higher morbidity from sepsis [44]. Poor prognosis is associated with a decreased OEF [26]. However, we found that OEF had a statistically significant increase in the CLP group, indicating that it might be a compensatory reaction to increase the resorption of oxygen in the early stage of sepsis. Overall, the Lac peak on MRS could reflect dysfunction of cerebral microcirculation.

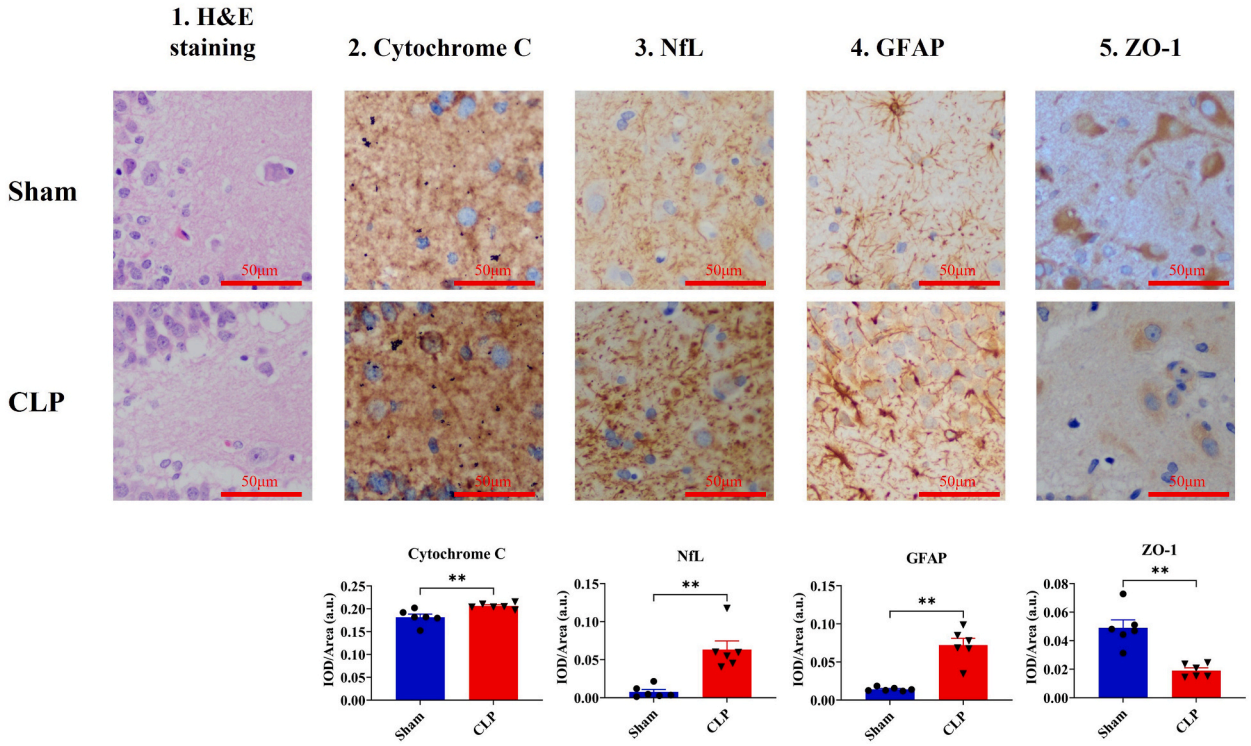

Fig. 4. Histopathological and immunohistochemical results for the subgroups M of the sham and CLP. The first panel (at far left) represents H&E staining of the sham and CLP subgroups M (× 400). There were no morphological alterations in the rats from the sham and CLP subgroups M. The following panels show protein markers in brain tissue detected by immunohistochemical staining and semi-quantitative indices (IOD/Area) in the sham and CLP subgroups M, as indicated by Cytochrome C (second panel), NfL (third panel), GFAP (fourth panel), and ZO-1 (fifth panel). Note: H&E staining = hematoxylin and eosin staining; CLP = cecal ligation and puncture; IOD/area = integrated optical density per stained area; NfL = neurofilament light chain; GFAP = glial fibrillary acidic protein; ZO-1, zonula occludens-1. *$p < 0.05$. **$p < 0.01$.

Citrate is an essential intermediate of energy metabolism that inhibits production of ATP from glycolysis and the tricarboxylic acid cycle (TCA), promotes the production of prostaglandins, reactive oxygen species (ROS), and nitric oxide, and exacerbates inflammation and cellular damage [16]. However, no statistically significant difference in citrate content between the two groups was shown in our results, which may be related to the fact that the established animal model of sepsis is still in its early stages, and renal function is still compensable. The kidney is the primary organ for the excretion of citrate [45]. Citrate is considerably elevated in patients with sepsis combined with renal insufficiency [46].

A compromised BBB may also contribute to the pathogenesis of SAE [2]. The lipid signals detected by 1H MRS were lipid droplets generated by cellular necrosis [20]. Upon exposure to damaging events, such as hypoxia, hypothermia, or inflammation, the cells become necrotic, thereby destroying the cell membrane [19]. Lipid droplets in the inbound state increase when the cell membrane is disrupted. Lip/Cr or Lip/NAA ratios serve as an affirmative indicator to judge the extent of brain injury [19]. An essential functional part of maintaining the blood–brain barrier is the tight junctions between endothelial cells composed of occludin and ZO-1 [47]. A higher organ failure score was correlated with the loss of expression of tight junction markers, which proved the breakdown of the BBB was involved in the development of sepsis [47]. In the present study we found that Lip/Cr was elevated in the unilateral hippocampal region of CLP-group rats and negatively correlated with the protein ZO-1, secondary to sepsis, suggesting that this concentration ratio could be used to assess SAE from the perspective of BBB integrity.

We chose a relatively early-stage sepsis model and performed MRI measurements at 12 h after CLP and functional neurological examination at 24, 48, and 72 h in subgroups. The experimental results suggested that neurological impairment is already present in rats starting 24 h after CLP. However, it is inconclusive as to exactly when MR can show brain abnormalities. Herein we chose to perform MR 12 h after CLP. We found that regular MR scanning did not allow early diagnosis, whereas MRS reflected metabolite differences between the two groups. MRS measurement was able to detect SAE early on, especially with respect to the changes in brain metabolism. In clinical practice, however, we have to deal with different stages of sepsis and different degrees of severity of sepsis. Many sepsis patients might experience a delay of at least 12 h after infection without treatment before presenting at a hospital. This is a reminder that in the future we can study MRI changes for different degrees of sepsis and whether intervention treatments (fluid resuscitation combined with antibiotics) produce MRI changes and improve prognosis.

The present study has confirmed MRS as a promising candidate for diagnosing sepsis-associated encephalopathy in a rat model of CLP. Compared with other methods, MRS combines multiple aspects to predict and evaluate cerebral injury in sepsis:

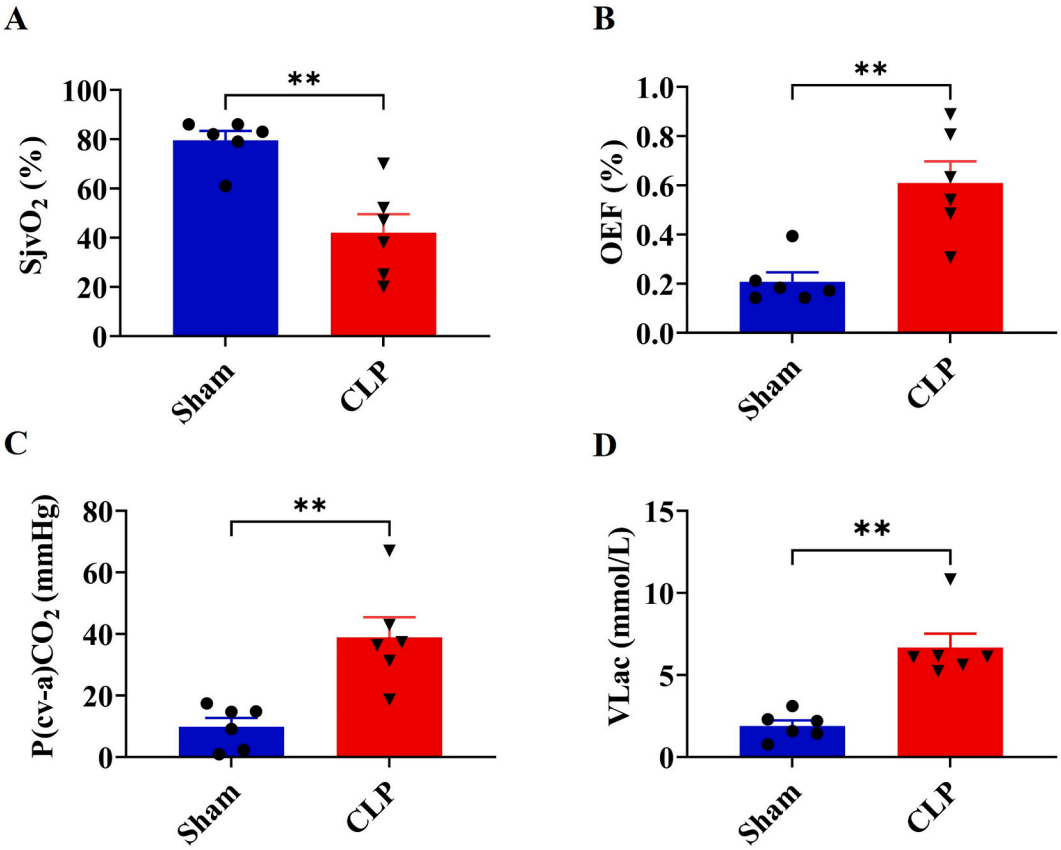

Fig. 5. Differences in blood gas analysis results between the sham and CLP subgroups M. $SjvO_2$ was lower in the CLP subgroup M compared with the sham subgroup M, while OEF, P (cv-a) CO_2 and VLac of the CLP subgroup M were higher than the corresponding values for the sham subgroup M. Note: CLP = cecal ligation and puncture; $SjvO_2$ = jugular venous oxygen saturation; OEF = oxygen extraction fraction; P (cv-a) CO_2 = central venous-to-arterial difference in carbon dioxide partial pressure; and VLac, venous blood lactate saturation. *$p < 0.05$. **$p < 0.01$.

neuroinflammation, oxidative stress, microcirculatory dysfunction, metabolic alteration, and blood–brain barrier disruption, which have particular specificity and sensitivity. We found that metabolic changes in the brain could be detected by MRS measurements as early as 12 h after CLP. Early identification leads to early intervention. Moreover, these metabolic changes can be further investigated as targets for preventing and treating SAE. It may therefore help us to intervene before morphological changes and neurological dysfunction occur. The development of diagnostic tools based on MRS will aid clinical monitoring of early brain injury due to SAE in patients and improve prognoses.

5. Limitations

Several limitations existed in our study. Firstly, the rat model of CLP does not always precisely replicate the actual situation of patients in the clinic. To begin with, the single sex and the single species limit translational relevance. Differences in gender or age may indeed affect the sepsis prognosis. We used animals of the same sex and age to minimize biological variability, but variation thereof deserves attention in future studies.

Secondly, we acknowledge that the absence of NDS measurement at 12 h in the MRS subgroup and the absence of MRI measurement at 24–72 h in the NDS subgroup are limitations of this study. However, the findings from OFT indicate that rats after CLP surgery exhibited diminished levels of total distance traveled and squares crossed, suggesting a decline in exploratory behaviour as well as reduced spontaneous activity and arousal.

Finally, our sample size was small, and we were unable to conduct correlation analysis or regression analysis of neural markers and quantitative MRS parameters. Despite this, our available experimental results, such as NDS scores, results of the OFT. immunohistochemical analyses, inflammatory factors, and blood gas analyses, were all consistent with MRS 12 h after CLP. It has thus been possible to demonstrate that MRS can quantitatively evaluate early SAE.

6. Conclusion

In the present study, 1H-MRS could be used to quantitatively assess brain injury in terms of microcirculation disorder, oxidative stress, blood–brain barrier disruption, and glial cell activation through changes in metabolites within brain tissue.

The underlying mechanism, reflected by metabolite changes seen through 1H-MRS, fits the experimental results from molecular biology. This approach may help provide a means of diagnosing and monitoring SAE patients and guide clinical policy-making.

Funding

This work was supported by the Natural Science Foundation of Guangdong Provincial Education Department (No. 2021A1515011433) and the National Natural Science Foundation of China (No. 82372207).

Data availability statement

Data will be made available on request.

CRediT authorship contribution statement

Siqi Liu: Writing – original draft, Software, Methodology, Investigation, Formal analysis. **Zhifeng Liu:** Writing – original draft, Software, Methodology, Investigation, Formal analysis. **Gongfa Wu:** Software, Methodology, Formal analysis. **Haoyi Ye:** Software, Methodology, Investigation. **Zhihua Wu:** Software, Methodology, Investigation, Formal analysis. **Zhengfei Yang:** Writing – review & editing, Supervision, Funding acquisition, Conceptualization. **Shanping Jiang:** Writing – review & editing, Supervision, Conceptualization.

Declaration of competing interest

The authors declare that they have no known competing financial interests or personal relationships that could have appeared to influence the work reported in this paper.

Appendix A. Supplementary data

Supplementary data to this article can be found online at https://doi.org/10.1016/j.heliyon.2024.e26836.

References

[1] M. Singer, C.S. Deutschman, C.W. Seymour, et al., The third international consensus definitions for sepsis and septic shock (Sepsis-3), JAMA 315 (8) (2016) 801–810.
[2] A. Mazeraud, C. Righy, E. Bouchereau, et al., Septic-associated encephalopathy: a comprehensive review, Neurotherapeutics 17 (2) (2020) 392–403.
[3] A.V. Catarina, G. Branchini, L. Bettoni, et al., Sepsis-associated encephalopathy: from pathophysiology to progress in experimental studies, Mol. Neurobiol. 58 (6) (2021) 2770–2779.
[4] A. Mazeraud, Q. Pascal, F. Verdonk, et al., Neuroanatomy and physiology of brain dysfunction in sepsis, Clin. Chest Med. 37 (2) (2016) 333–345.
[5] T.E. Gofton, G.B. Young, Sepsis-associated encephalopathy, Nat. Rev. Neurol. 8 (10) (2012) 557–566.
[6] K. Hosokawa, N. Gaspard, F. Su, et al., Clinical neurophysiological assessment of sepsis-associated brain dysfunction: a systematic review, Crit. Care 18 (6) (2014) 674.
[7] S.C. Tauber, M. Djukic, J. Gossner, et al., Sepsis-associated encephalopathy and septic encephalitis: an update, Expert Rev. Anti Infect. Ther. 19 (2) (2021) 215–231.
[8] M. Wen, Z. Lian, L. Huang, et al., Magnetic resonance spectroscopy for assessment of brain injury in the rat model of sepsis, Exp. Ther. Med. 14 (5) (2017) 4118–4124.
[9] F.A. Bozza, P. Garteiser, M.F. Oliveira, et al., Sepsis-associated encephalopathy: a magnetic resonance imaging and spectroscopy study, J. Cerebr. Blood Flow Metabol. 30 (2) (2010) 440–448.
[10] N. Mazibuko, R.O.G. Tuura, L. Sztriha, et al., Subacute changes in *N*-acetylaspartate (NAA) following ischemic stroke: a serial MR spectroscopy pilot study, Diagnostics 10 (7) (2020) 482.
[11] V. Veeramuthu, P. Seow, V. Narayanan, et al., Neurometabolites alteration in the acute phase of mild traumatic brain injury (mTBI): an in vivo proton magnetic resonance spectroscopy (1H-MRS) study, Acad. Radiol. 25 (9) (2018) 1167–1177.
[12] C.D. Rae, A guide to the metabolic pathways and function of metabolites observed in human brain 1H magnetic resonance spectra, Neurochem. Res. 39 (1) (2014) 1–36.
[13] N.A. Sibtain, F.A. Howe, D.E. Saunders, The clinical value of proton magnetic resonance spectroscopy in adult brain tumours, Clin. Radiol. 62 (2) (2007) 109–119.
[14] J. Zhang, S. Liu, L. Jiang, et al., Curcumin improves cardiopulmonary resuscitation outcomes by modulating mitochondrial metabolism and apoptosis in a rat model of cardiac arrest, Frontiers in cardiovascular medicine 9 (2022) 908755.
[15] F.A. Bozza, J.C. D'Avila, C. Ritter, et al., Bioenergetics, mitochondrial dysfunction, and oxidative stress in the pathophysiology of septic encephalopathy, Shock 39 (Suppl 1) (2013) 10–16.
[16] H. Jaurila, V. Koivukangas, M. Koskela, et al., ^{1}H NMR based metabolomics in human sepsis and healthy serum, Metabolites 10 (2) (2020) 70.
[17] X. Zhai, Z. Yang, G. Zheng, et al., Lactate as a potential biomarker of sepsis in a rat cecal ligation and puncture model, Mediat. Inflamm. 2018 (2018) 8352727.
[18] A.S. Kierans, I.I. Kirov, O. Gonen, et al., Myoinositol and glutamate complex neurometabolite abnormality after mild traumatic brain injury, Neurology 82 (6) (2014) 521–528.

[19] Y.H. Jung, H. Kim, S.Y. Jeon, et al., Brain metabolites and peripheral biomarkers associated with neuroinflammation in complex regional pain syndrome using [11C]-(R)-PK11195 positron emission tomography and magnetic resonance spectroscopy: a pilot study, Pain Med. 20 (3) (2019) 504–514.
[20] S. Zoula, G. Hérigault, A. Ziegler, et al., Correlation between the occurrence of 1H-MRS lipid signal, necrosis and lipid droplets during C6 rat glioma development, NMR Biomed. 16 (4) (2003) 199–212.
[21] J.D. Clark, G.F. Gebhart, J.C. Gonder, et al., Special report: the 1996 guide for the care and use of laboratory animals, ILAR J. 38 (1) (1997) 41–48.
[22] L.C. Alworth, S.B. Harvey, IACUC issues associated with amphibian research, ILAR J. 48 (3) (2007) 278–289.
[23] K.A. Wichterman, A.E. Baue, I.H. Chaudry, Sepsis and septic shock–a review of laboratory models and a proposal, J. Surg. Res. 29 (2) (1980) 189–201.
[24] E.M. Nemoto, A.L. Bleyaert, S.W. Stezoski, et al., Global brain ischemia: a reproducible monkey model, Stroke 8 (5) (1977) 558–564.
[25] L. Prut, C. Belzung, The open field as a paradigm to measure the effects of drugs on anxiety-like behaviors: a review, Eur. J. Pharmacol. 463 (1–3) (2003).
[26] T. Nakamura, N. Tatara, K. Morisaki, et al., Cerebral oxygen metabolism monitoring under hypothermia for severe subarachnoid hemorrhage: report of eight cases, Acta Neurol. Scand. 106 (5) (2002) 314–318.
[27] A.M. Lucke, A.N. Shetty, J.L. Hagan, et al., Early proton magnetic resonance spectroscopy during and after therapeutic hypothermia in perinatal hypoxic-ischemic encephalopathy, Pediatr. Radiol. 49 (7) (2019) 941–950.
[28] A. Eisele, M. Hill-Strathy, L. Michels, et al., Magnetic resonance spectroscopy following mild traumatic brain injury: a systematic review and meta-analysis on the potential to detect posttraumatic neurodegeneration, Neurodegener. Dis. 20 (1) (2020) 2–11.
[29] G. Paslakis, F. Träber, J. Roberz, et al., N-acetyl-aspartate (NAA) as a correlate of pharmacological treatment in psychiatric disorders: a systematic review, Eur. Neuropsychopharmacol 24 (10) (2014) 1659–1675.
[30] J.R. Moffett, B. Ross, P. Arun, et al., N-Acetylaspartate in the CNS: from neurodiagnostics to neurobiology, Prog. Neurobiol. 81 (2) (2007) 89–131.
[31] J.A. Calvar, F.J. Meli, C. Romero, et al., Characterization of brain tumors by MRS, DWI and Ki-67 labeling index, J. Neuro Oncol. 72 (3) (2005) 273–280.
[32] S. Currie, M. Hadjivassiliou, I.J. Craven, et al., Magnetic resonance spectroscopy of the brain, Postgrad. Med. 89 (1048) (2013) 94–106.
[33] D.M. Norden, P.J. Trojanowski, E. Villanueva, et al., Sequential activation of microglia and astrocyte cytokine expression precedes increased Iba-1 or GFAP immunoreactivity following systemic immune challenge, Glia 64 (2) (2016) 300–316.
[34] M. Savran, O. Ozmen, Y. Erzurumlu, et al., The impact of prophylactic lacosamide on LPS-Induced neuroinflammation in aged rats, Inflammation 42 (5) (2019) 1913–1924.
[35] L.-D. Niu, W. Xu, J.-Q. Li, et al., Genome-wide association study of cerebrospinal fluid neurofilament light levels in non-demented elders, Ann. Transl. Med. 7 (22) (2019) 657.
[36] Z. Yang, K.K.W. Wang, Glial fibrillary acidic protein: from intermediate filament assembly and gliosis to neurobiomarker, Trends Neurosci. 38 (6) (2015) 364–374.
[37] J. Warford, A.-C. Lamport, B. Kennedy, et al., Human brain chemokine and cytokine expression in sepsis: a report of three cases, Can. J. Neurol. Sci. 44 (1) (2017) 96–104.
[38] C. Ince, The microcirculation is the motor of sepsis, Crit. Care 9 (Suppl 4) (2005) S13–S19.
[39] R. Sonneville, F. Verdonk, C. Rauturier, et al., Understanding brain dysfunction in sepsis, Ann. Intensive Care 3 (1) (2013) 15.
[40] A. Matsumura, T. Isobe, S. Takano, et al., Non-invasive quantification of lactate by proton MR spectroscopy and its clinical applications, Clin. Neurol. Neurosurg. 107 (5) (2005) 379–384.
[41] D.D.M. Lin, T.O. Crawford, P.B. Barker, Proton MR spectroscopy in the diagnostic evaluation of suspected mitochondrial disease, AJNR Am J Neuroradiol 24 (1) (2003) 33–41.
[42] W.J. Hubbard, K.I. Bland, I.H. Chaudry, The role of the mitochondrion in trauma and shock, Shock 22 (5) (2004) 395–402.
[43] J. Richter, P. Sklienka, A.E. Setra, et al., Is jugular bulb oximetry monitoring associated with outcome in out of hospital cardiac arrest patients? J. Clin. Monit. Comput. 35 (4) (2021) 741–748.
[44] L. Alegria, M. Vera, J. Dreyse, et al., A hypoperfusion context may aid to interpret hyperlactatemia in sepsis-3 septic shock patients: a proof-of-concept study, Ann. Intensive Care 7 (1) (2017) 29.
[45] L.C. Costello, R.B. Franklin, Plasma citrate homeostasis: how it is regulated; and its physiological and clinical implications. An important, but neglected, relationship in medicine, HSOA J Hum Endocrinol 1 (1) (2016) 5.
[46] S. Singh, T. Chatterji, M. Sen, et al., Serum procalcitonin levels in combination with (1)H NMR spectroscopy: a rapid indicator for differentiation of urosepsis, Clin. Chim. Acta 453 (2016) 205–214.
[47] K. Erikson, H. Tuominen, M. Vakkala, et al., Brain tight junction protein expression in sepsis in an autopsy series, Crit. Care 24 (1) (2020) 385.